The Structural Plasticity of the C Terminus of p21Cip1 is a Determinant for Target Protein Recognition

ARTICLE *in* CHEMBIOCHEM · SEPTEMBER 2003

Impact Factor: 3.09 · DOI: 10.1002/cbic.200300649 · Source: PubMed

The Structural Plasticity of the C Terminus of p21^{Cip1} is a Determinant for Target Protein Recognition

Vicent Esteve,[a, d] Núria Canela,[b] Aina Rodriguez-Vilarrupla,[b] Rosa Aligué,[b] Neus Agell,[b] Ismael Mingarro,[a] Oriol Bachs,[b] and Enrique Pérez-Payá*[a, c]

The cyclin-dependent kinase inhibitory protein p21^{Cip1} might play multiple roles in cell-cycle regulation through interaction of its C-terminal domain with a defined set of cellular proteins such as proliferating cell nuclear antigen (PCNA), calmodulin (CaM), and the oncoprotein SET. p21^{Cip1} could be described as an intrinsically unstructured protein in solution although the C-terminal domain adopts a well-defined extended conformation when bound to PCNA. However, the molecular mechanism of the interaction with CaM and the oncoprotein SET is not well understood, partly because of the lack of structural information. In this work, a peptide derived from the C-terminal domain of p21^{Cip1} that covers the binding domain of the three above-mentioned proteins was used to demonstrate that the C-terminal domain of p21 recognizes multiple ligands through its ability to adopt multiple conformations. The conformation is dictated by tertiary contacts rather than by the primary sequence of the protein. Our results suggest that the C-terminal domain of p21^{Cip1} adopts an extended structure when bound to PCNA and probably when bound to the oncoprotein SET, but an α helix when bound to CaM.

KEYWORDS:

conformation analysis · molecular recognition · peptides · proteins · structural plasticity

Introduction

Cell-cycle progression is driven by a family of serine-threonine kinases named cyclin-dependent kinases (CDKs). CDK activity is regulated by a variety of mechanisms, including association with regulatory subunits named cyclins, phosphorylation of positive and negative regulatory sites, and binding to a number of proteins called CDK inhibitors.[1] One of these kinase inhibitors, the p21^{Cip1} (p21) protein, was originally identified as a CDK and proliferating cell nuclear antigen (PCNA)-binding protein and as a gene product whose expression is induced by the tumor suppressor protein p53.[2–4] Initially, p21 was considered a general inhibitor of most cyclin – CDK complexes and, when bound to PCNA, an inhibitor of DNA synthesis.

More recently, it has become clear that p21 might play multiple roles in cell-cycle regulation. These include mediation of negative regulatory signals, differentiation and senescence, modulation of apoptosis, and activation of certain cyclin – CDK complexes.[5, 6] Whereas p21 is a potent inhibitor of CDK2-containing complexes, it stimulates the assembly of active cyclin D1 – CDK4 complexes and targets their nuclear localization.[7] These functions are performed by the N-terminal half of the molecule, which contains a cyclin-binding motif (aa 16 – 24) and a CDK interaction site (aa 45 – 65).[8]

The whole p21 protein and its kinase inhibitory N-terminal domain are soluble and stable in solution but no evidence has been found by nuclear magnetic resonance (NMR) or circular dichroism (CD) spectroscopies of the presence of secondary or tertiary structure.[9] However, it has been shown by NMR spectroscopy that the kinase inhibitory domain adopts an ordered conformation when bound to CDK2.[9]

The C terminus of p21 contains a domain that interacts with PCNA (aa 144 – 151), and a putative nuclear localization signal (aa 140 – 143).[8, 10] More recently, it has been reported that calmodulin (CaM) and the oncoprotein SET are also target proteins that bind to the C terminus of p21 (aa 145 – 164).[11, 12] Whereas CaM binds to this domain in a Ca^{2+}-dependent manner, the binding of SET and PCNA does not depend on Ca^{2+} concentration.

[a] *Dr. E. Pérez-Payá, Dr. V. Esteve, Dr. I. Mingarro*
Dept. Bioquímica i Biologia Molecular
Universitat de València
46100 Burjassot, València (Spain)
Fax: (+34) 9635-44635
E-mail: paya@uv.es

[b] *Dr. N. Canela, A. Rodriguez-Vilarrupla, Dr. R. Aligué, Dr. N. Agell, Prof. Dr. O. Bachs*
Dept. Biologia Cellular i Anatomia Patològica
Facultat de Medicina
Institut d'Investigacions Biomèdiques August Pi Sunyer
Universitat de Barcelona, 08036 Barcelona (Spain)

[c] *Dr. E. Pérez-Payá*
Dept. Química Orgànica Biologica
I.I.Q.A.B. (C.S.I.C.), 08034 Barcelona (Spain)

[d] *Dr. V. Esteve*
Present address:
Institute of Molecular Biology and Biophysics
ETH Hönggerberg, 8093 Zürich (Switzerland)

 DOI: 10.1002/cbic.200300649

The crystal structure of human PCNA complexed with a peptide corresponding to the 22 C-terminal residues of p21 has been reported.[13] p21 binds to PCNA in a 1:1 stoichiometry with interactions that include the formation of an extended β sheet with the interdomain connector loop of PCNA. In contrast, there is no structural information on the putative complexes that p21 forms with CaM and SET. However, it is recognized that when CaM binds to CaM-binding proteins, the binding domain of these proteins is induced to fold into an amphipathic α helix.[14–18] In this sense, the ability of the C-terminal domain of p21 to recognize different proteins could be derived not only from the complementarity of preformed protein surfaces, but rather from the ability of p21 to adopt multiple conformations that mediate diverse binding events.

Different macromolecule binding pockets may dictate distinct conformations of the same polypeptide. There are now many known examples of proteins that have the ability to associate with multiple ligands by using essentially the same set of surface residues, which allows a single molecular surface to interact with different structurally distinct binding partners.[19–21] In this context, we questioned whether a peptide ($p21^{145–164}$) that lacks stable secondary structure in free solution[9] and adopts an extended structure when bound to one protein (PCNA[13]), could adapt its conformation when bound to a different protein (CaM[11]) that recognizes only α-helical structures in its target proteins.[14–17] It can be anticipated that the folding of a given peptide from an initial random coil in solution into a low-energy, highly ordered bound conformation would be dependent on the target protein environment and on intrinsic peptide plasticity. In the absence of high-resolution structural data for the peptide–target protein complex, the peptide conformational plasticity can be studied by means of CD and NMR spectroscopies in the presence of solvents with well-known properties that induce secondary structure in peptides.

We report herein the results of biophysical studies aimed at understanding the role of the induced conformational changes on the C-terminal domain of p21 upon binding to the target protein interface. The conformational plasticity of this domain confers to p21 the ability to bind to multiple proteins by using essentially the same set of surface residues. The versatility of the C-terminal domain of p21 appears to stem from the flexible use of an amino acid sequence that does not have any clear secondary structure propensity in isolation and will adopt a secondary structure determined by the characteristics of the target proteins. Our results, in fact, suggest that the C-terminal domain of p21 adopts an extended structure when bound to PCNA and probably when bound to the SET protein, but an α helix when bound to CaM.

Results

Identification of $p21^{145–164}$ as the p21 domain responsible for binding to PCNA, to CaM, and to the oncoprotein SET

In our previous studies on the binding of p21 to CaM and to the oncoprotein SET[11, 12, 22] we performed pull-down experiments by using three peptides corresponding to different regions of the p21 molecule. The peptide $p21^{145–164}$ (p21 sequence numbering) was shown to define the domain of p21 that binds to both CaM and to the SET protein. The PCNA-binding functionality of p21 was defined early-on as residing in the C-terminal 22 residues of the protein, which also suffice to block PCNA-mediated DNA replication.[13] The peptide $p21^{139–160}$ was found to bind to human PCNA with high affinity and inhibits DNA synthesis in vitro.[23, 24]

The peptide $p21^{145–164}$, derived from the CaM-, PCNA-, and SET-binding domain of p21, was synthesized with the extrinsic fluorescent probe dansyl (DNS) attached to the N terminus (DNS–$p21^{145–164}$) to allow us to examine its affinity for the three different proteins in a fluorescence study. Extrinsic fluorescent probes are well-suited for this purpose because their excitation wavelength is different from those of intrinsic aromatic amino acids and their emission wavelengths are sensitive to the environment. The relative binding affinity of DNS–$p21^{145–164}$ for CaM, PCNA, and SET was determined by titration of peptide solutions with increasing concentrations of each protein in the presence and in the absence of Ca^{2+}. When the dansyl group of free DNS–$p21^{145–164}$ is selectively excited at 330 nm, an emission maximum (λ_{max}) is observed at 518 nm. The fluorescence of the DNS–$p21^{145–164}$ peptide is sensitive to protein binding. The binding curves to each protein (Figure 1) are monophasic, very

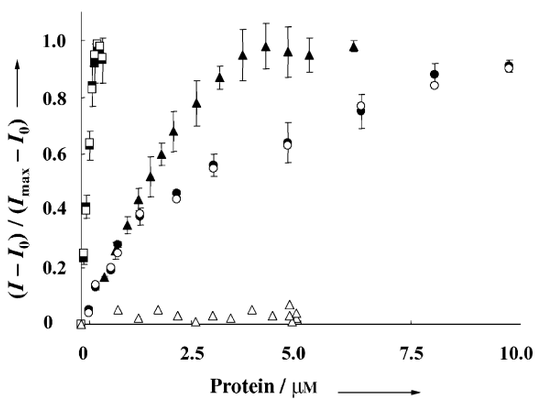

Figure 1. *Binding of the proteins CaM (triangles), PCNA (circles), and SET (squares) to DNS–$p21^{145–164}$ over a range of protein concentrations in the presence (full symbols) and in the absence (empty symbols) of 5 mM $CaCl_2$, as measured by the relative fluorescence intensity (see the Materials and Methods Section) of the dansyl fluorescent probe.*

similar in shape, and they reach a plateau at different protein/peptide concentration ratios. We obtained different values for λ_{max} and for the relative increase in fluorescence intensity (F_R—see the Materials and Methods Section) for each protein in the bound state (Table 1). These results suggest that the fluorescent probe is more exposed to solvent when bound to PCNA and SET than when bound to CaM. The binding of DNS–$p21^{145–164}$ to CaM is Ca^{2+} dependent (Figure 1), however the peptide binds to PCNA and SET protein in the presence or absence of Ca^{2+} with identical binding affinity constants. By analysis of the binding curves,[25] it could be derived that DNS–$p21^{145–164}$ binds to CaM,

Table 1. *Fluorescence parameters of DNS – p21[145–164] in the free and bound states.[a]*

	Free in solution	CaM	PCNA	SET
λ_{max} [nm][b]	518	492	502	508
F_R[c]	1	5.8	2.9	4.2

[a] The fluorescence parameters were obtained from the fluorescence emission spectra of DNS – p21[145–164] in the absence (free) and in the presence of a saturating concentration of each protein (bound state, see text and Figure 1). [b] The wavelength maximum for each spectrum was estimated by measuring the wavelength of the mid-point at two-thirds the height of the spectral band.[39] [c] Relative fluorescence intensity (F_R) values were calculated as the ratio between the fluorescence emission maximum of the spectrum for the bound state and the same value of the spectrum obtained for the peptide in the absence of protein.

PCNA, and SET with stoichiometry (peptide:protein) and apparent dissociation constants ($K_{d,app}$) of 1:1, $K_{d,app} = 1.7 \times 10^{-6}$ M; 2:1, $K_{d,app} = 2.4 \times 10^{-6}$ M; and 10:1, $K_{d,app} = 1.6 \times 10^{-7}$ M, respectively. The data obtained for the interaction between DNS – p21[145–164] and PCNA are consistent with data reported previously on the interaction p21 – PCNA,[13, 24] within the error boundaries of the experiments. In these previous works, the dissociation constant for the peptide p21[141–160] was accurately determined by means of isothermal titration calorimetry to be 8.8×10^{-8} M with a stoichiometry of 1:1, which is confirmed by the crystal structure of the complex.

Structural characterization of the p21[145–164] peptide in different environments

The ability of a polypeptide sequence to populate different conformational spaces when bound to different proteins, structural changes which in vivo should be triggered by the target protein, can be analyzed in vitro by means of conformational analysis in the presence of secondary structure inducers.

We determined the solution structure of the p21[145–164] peptide in plain buffered solutions and in the presence of 2,2,2-trifluoroethanol (TFE) and sodium dodecyl sulfate (SDS). The CD spectra of the peptide show an unordered structure (Figure 2A). Similar results have been obtained for a synthetic peptide that covers the 39 C-terminal amino acids of p21.[26] In order to assay the propensity of the peptide to be induced to form a defined secondary structure, the CD spectra were also recorded in the presence of TFE, a solvent known to induce helicity in single-stranded potentially α-helical polypeptides,[27] or in submicellar concentrations of SDS, which is considered a template that would stabilize β-sheet conformations depending on the polypeptide microenvironment.[27, 28] At TFE concentrations as low as 20%, p21[145–164] was induced to form an α helix (Figure 2A). In the presence of 1.5 mM SDS, however, the peptide was induced to fold into a β-sheet conformation (Figure 2A). Increased concentrations of TFE further stabilized the α-helical conformation and the presence of an isodichroic point at 204 nm suggests that no significant portion of the peptide molecules present in the solution populate conformations other than the random coil and α helix. In contrast, the conformational behavior

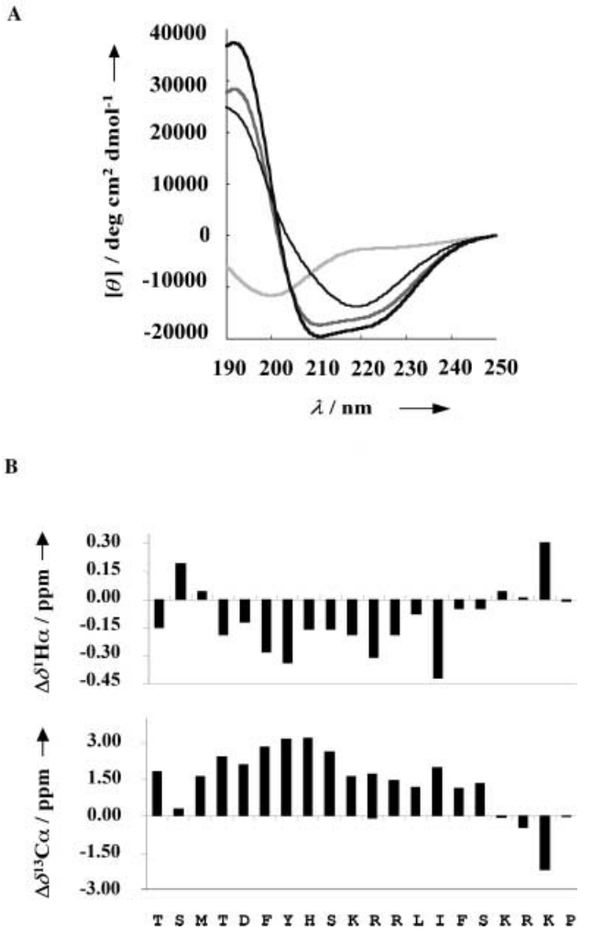

Figure 2. *Structural characterization of the p21[145–164] peptide in different environments. A) Far-UV CD spectra of the peptide at a concentration of 50 μM in 5 mM MOPS/NaOH, 120 mM NaCl, pH 7.0 (light grey line); in the presence of 20% TFE (medium grey line); 40% TFE (black line); and in the presence of 1.5 mM SDS (thin black line). B) NMR analysis of the peptide in the presence of 20% TFE. Observed conformational chemical shift increments for ^{1}H ($\Delta\delta^1$Hα) and for ^{13}C ($\Delta\delta^{13}$Cα) relative to the chemical shifts of random peptides. The one-letter code for the amino acids is used for the peptide sequence on the x axis.*

in the presence of increasing concentrations of SDS is more complex. When SDS is present in the solution as a monomer (SDS concentrations below the critical micellar concentration, cmc) the peptide is stabilized in a β-sheet conformation (Figure 2A). However, when SDS is in a micellar form (SDS concentrations above the cmc) the energetically stabilized conformation is an α helix (data not shown).

The NMR spectra for the peptide p21[145–164] were recorded in aqueous solution and in 20% TFE. Unfortunately, at the high peptide concentrations required for NMR spectroscopy, the presence of low concentrations of SDS induced unspecific aggregation that precluded NMR analysis under these conditions. Sequential assignments were obtained from the "fingerprint" region of the two-dimensional TOCSY, ROESY, and NOESY spectra as previously described.[29] The adoption of a defined preferential secondary structure by a peptide induces significant

and specific chemical shift changes in both ^{1}H and ^{13}C nuclei that can be used to quantify secondary structure populations. In particular, an α-helical conformation is characterized by upfield and downfield shifts of the H_α and C_α nuclei, respectively. Therefore, one can measure the deviation of the experimental chemical shifts from those attributed to random coil conformation for each residue to analyse the conformation of the peptide.[30] The peptide adopts a random structure (data not shown) in buffered solution. However, the polypeptide appeared to populate an α-helical conformation in 20% TFE solution, as defined by the analysis of the conformational chemical shifts of $^{1}H_\alpha$ and $^{13}C_\alpha$ (Figure 2B) and by the presence of H_α-NH NOE connectivities between the residues Ser146 – Asp149, Ser146 – Phe150, Met147 – Phe150, Thr148 – Tyr151, Ser153 – Arg156, and Arg155 – Phe159.

An extended structure at the C terminus of p21 is required for binding to PCNA and SET but not to CaM

We have seen that the C-terminal peptide of p21, $p21^{145–164}$, can adopt different conformations depending on the environment. The peptide, disordered in aqueous solution, folds into an amphipathic α helix in the presence of TFE (Figures 2 and 3A) and into an extended β-sheet conformation in the presence of monomeric SDS (Figure 2A). It has been reported that the extended conformation is also induced when the peptide is bound to PCNA. Residues His152 to Ser160 form a β sheet with the interdomain connector loop of PCNA and residues Ser146 to Tyr151 are folded into a short 3_{10} helix (Figure 3B) that adapts to fit a hydrophobic pocket present in PCNA.[13]

To further corroborate the importance of the structural plasticity of the p21 C-terminal sequence upon binding to the target proteins, we designed a $p21^{145–164}$ mutant peptide with restricted structural plasticity. Thus, peptide $(PK)_2p21^{145–164}$ (Figure 3C) has a four amino acid replacement at the N terminus (Ser146Pro, Met147Lys, Asp149Pro, and Phe150Lys) that precludes induction of an amphipathic α-helical conformation but can still be induced to fold into an extended β-sheet conformation from residue His152 to Ser160. The peptide was used in pull-down experiments to determine whether or not it is able to bind to the p21 target proteins analyzed in this work. The results suggested that PCNA and SET were able to bind to the mutant peptide (Figure 4A). In contrast, as expected from its binding

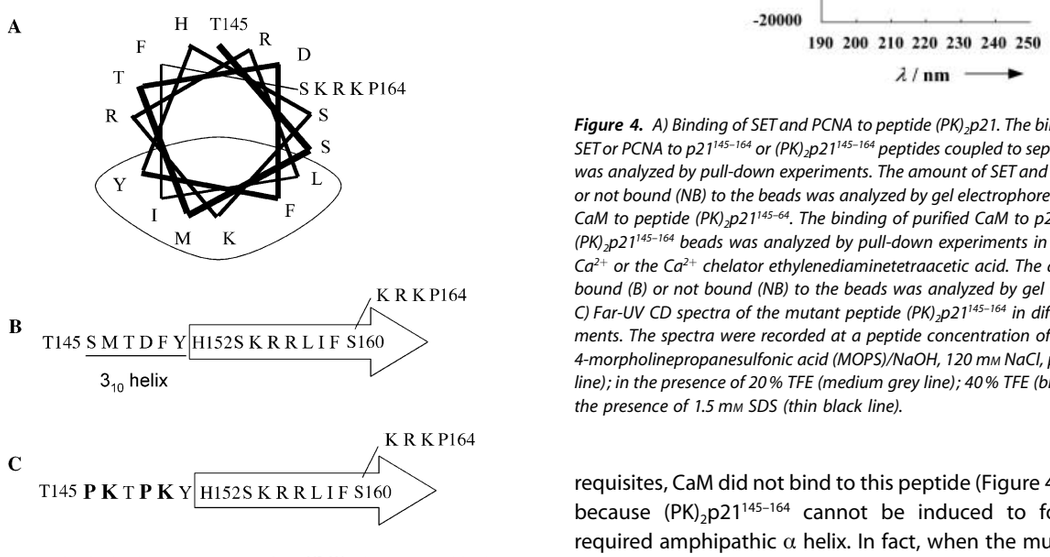

Figure 3. A) Helical wheel representation of $p21^{145–164}$. The proposed hydrophobic face of the helix is circled. B) Schematic depiction of the conformation adopted by $p21^{145–164}$ when bound to PCNA, adapted from ref. [13] C) Schematic representation of the mutant peptide $(PK)_2p21^{145–164}$ in a putative extended conformation.

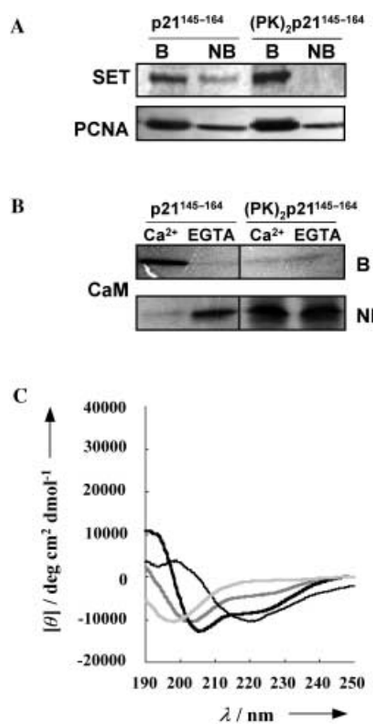

Figure 4. A) Binding of SET and PCNA to peptide $(PK)_2p21$. The binding of purified SET or PCNA to $p21^{145–164}$ or $(PK)_2p21^{145–164}$ peptides coupled to sepharose 4B beads was analyzed by pull-down experiments. The amount of SET and PCNA bound (B) or not bound (NB) to the beads was analyzed by gel electrophoresis. B) Binding of CaM to peptide $(PK)_2p21^{145–64}$. The binding of purified CaM to $p21^{145–164}$ or $(PK)_2p21^{145–164}$ beads was analyzed by pull-down experiments in the presence of Ca^{2+} or the Ca^{2+} chelator ethylenediaminetetraacetic acid. The amount of CaM bound (B) or not bound (NB) to the beads was analyzed by gel electrophoresis. C) Far-UV CD spectra of the mutant peptide $(PK)_2p21^{145–164}$ in different environments. The spectra were recorded at a peptide concentration of 50 μM in 5 mM 4-morpholinepropanesulfonic acid (MOPS)/NaOH, 120 mM NaCl, pH 7.0 (light grey line); in the presence of 20% TFE (medium grey line); 40% TFE (black line); and in the presence of 1.5 mM SDS (thin black line).

requisites, CaM did not bind to this peptide (Figure 4B), probably because $(PK)_2p21^{145–164}$ cannot be induced to fold into the required amphipathic α helix. In fact, when the mutant peptide was analyzed by CD spectroscopy (Figure 4C) the results showed that the peptide has a random conformation in buffer and a highly diminished ability, when compared to the original $p21^{145–164}$ peptide, to fold into an α helix in the presence of

TFE. Interestingly enough, the peptide showed the finger-print CD spectra of a β-sheet conformation in the presence of 1.5 mM SDS.

Discussion

The cell cycle receives and integrates signals from diverse growth regulatory pathways ensuring that the cell grows only in the presence of the appropriate signals. Cell-cycle progression is driven by CDKs that in addition receive and integrate the growth regulatory signals that are targeted to the cell cycle. The CDK inhibitor p21 negatively regulates cell-cycle progression and enforces a cell-cycle arrest when over-expressed in a cell.[3, 31] In addition, p21 has long been known to bind to PCNA and more recently it was found to bind many other regulatory proteins,[32] in particular CaM and SET.[11, 12] Given the increasing number of proteins reported to bind to p21 and the fact that the protein is highly disordered in the absence of a defined target protein,[9, 33] it is plausible that binding to the target proteins relies on the structural plasticity of p21, which confers upon it the ability to adapt to different recognition motifs.

The N-terminal domain of p21 contains the kinase inhibitory domain and undergoes a disorder-to-order transition upon binding to CDK2.[9] Furthermore, we have shown here that a 20-mer peptide ($p21^{145–164}$) from the C-terminal domain of p21 is disordered in solution although the peptide can be easily induced to fold into different secondary structures depending on the environment. Low TFE concentrations induced an α-helical conformation while monomeric SDS induced a β-sheet conformation. The ability of the $p21^{145–164}$ peptide to be stabilized in different conformations could explain how this peptide is able to bind to PCNA in an extended structure (Figure 5 A)[13] as well as to CaM, which only binds to α-helical peptides.[14–18] Although the detailed structure of the $p21^{145–164}$–CaM complex is not available at the moment, a model structure was obtained by using the CHARMM molecular modeling program. Initially, the $p21^{145–164}$ peptide was modeled to fold into a canonical α-helical conformation (see the Materials and Methods section). Figure 5 B shows the superposition of the α-helical conformations obtained for modeled $p21^{145–164}$ and the myosin light chain kinase (MLCK) peptide (see the Materials and Methods section). The $p21^{145–164}$–CaM complex (Figure 5 C) was generated by superimposing the α-helical conformations of the constructed $p21^{145–164}$ model and the MLCK peptide to form the complex MLCK–CaM in such a way that the two Phe residues, present and equidistant in the two peptides, are aligned. The output of the model suggests that the $p21^{145–164}$ peptide could fit into the CaM binding groove in a similar way to other CaM-binding peptides.[34] The interaction between CaM and p21 could be related to the nuclear translocation of p21. It has been shown that CaM is essential to induce translocation of p21 to the cell nucleus[11] and we are currently exploring the hypothesis that the binding of CaM to $p21^{145–164}$ could be used to expose the nuclear localization sequence necessary for translocation.[10]

The cellular role of the oncoprotein SET is still an open question. SET interacts specifically with B-type cyclins but not with cyclin A[35] and we recently reported that this binding of SET to cyclin B inhibits cyclin B–CDK1 activity.[22] SET has been found to be identical to template-activating factor Iβ (TAF-Iβ), a host protein necessary for DNA replication of the adenovirus

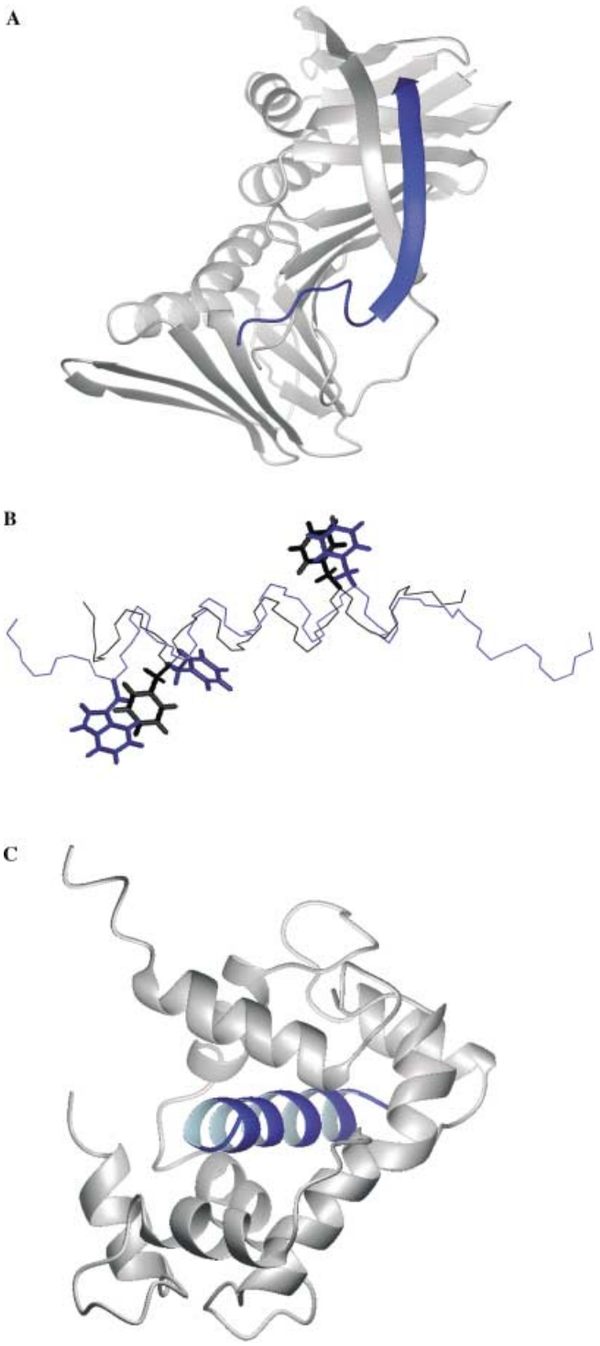

Figure 5. *A) Ribbon diagram of the PCNA monomer (grey) with bound p21 peptide (blue), adapted from ref. [13] B) Superposition of the backbone α-helical conformations obtained for $p21^{145–164}$ (black) and for the conformation of the 26-residue synthetic MLCK peptide (blue) when bound to CaM (see the text for details). The side chains of Trp4, Phe8, and Phe17 from MLCK that fit into hydrophobic pockets of CaM,[34] and Phe150 and Phe159 from $p21^{145–164}$ are depicted. C) Cartoon of the modeled $p21^{145–164}$(blue)–CaM (grey) complex.*

genome.[36] The structure of TAF-I has not been solved at atomic resolution although it has been shown that the protein isolated from HeLa cells exists as a dimer.[37] It has been proposed that the dimerization motif resides in the N-terminal region of the protein, which shows a high probability for formation of α-helical coiled-coil structure.[37] The C-terminal domain of SET/TAF-I is characterized by the presence of a long acidic tail predicted to adopt a random structure under physiological conditions. We have recently found that this acidic C-terminal domain of SET binds to $p21^{145-164}$; however, another binding domain is also present in the central region of SET (aa 81–180).[22] Complex formation would induce the stabilization of a β-sheet conformation in the C-terminal domain of p21. Two lines of evidence support such a hypothesis. First, the fluorescence spectrum of DNS–$p21^{145-164}$ bound to SET shows a λ_{max} value (Table 1) that suggests a partially solvent-exposed location similar to that obtained for the peptide bound to PCNA, which has been shown to bind to the surface of the protein.[13] Second, the SET protein binds to the mutant peptide $(PK)_2p21^{145-164}$ (Figure 4A), which has been demonstrated to retain the ability of the original $p21^{145-164}$ peptide to be induced to fold into a β-sheet conformation but not into an α-helical conformation (Figure 4B).

In conclusion, our data suggest that the C-terminal domain of p21 recognizes multiple ligands through its ability to adopt multiple conformations dictated by tertiary contacts rather than by its primary sequence. This may allow p21 to interact with a diverse set of proteins during the process of cell-cycle progression. Our study provides insights into how this flexible module may control multiple molecular events leading to the control of cell growth and replication. These results reinforce the view that the lack of a regular backbone fold in intrinsically unstructured proteins can allow the backbone to serve as a molecular scaffold for a broad range of intermolecular interactions.

Materials and Methods

Materials: Deuterium oxide (^2H_2O) and d_3-TFE were obtained from Cambridge Isotopes Labs (Cambridge, UK). All other chemicals were purchased from standard suppliers. The peptides used in the study described herein were synthesized at the peptide synthesis facility of the University of Barcelona.

Expression and purification of recombinant proteins: A pGEX-KG vector containing SET, and the PET vector containing the PCNA-His tag were transformed into BL21(DE3)-strain *Escherichia coli* carrying the pLysS plasmid. Expression and purification of the proteins were performed as previously described by using glutathione-affinity[12] or Ni-affinity chromatography according to the manufacturer recommendations (Novagen). Glutathione-S transferase (GST) was cut off from SET by digestion with thrombin protease according to the manufacturer recommendations (Sigma). Human recombinant CaM was also expressed in *Escherichia coli* and purified as previously described.[38]

Pull-down experiments: Pull-down experiments were performed as previously described.[11] Peptides $p21^{145-164}$ and $(PK)_2p21^{145-164}$ were coupled to BrCN-activated sepharose 4B (Amersham Pharmacia Biotech), as indicated by the manufacturer. Samples (1–4 μg protein) were incubated with immobilized peptides (2 μg) in the binding buffer (50 mM tris(hydroxymethyl)aminomethane (Tris)-HCl, pH 7.4, 150 mM NaCl, 1 mM dithiothreitol, 1% Triton X-100) for 2 h at room temperature. The beads were then extensively washed with binding buffer. The unbound fraction was the supernatant of the first wash. The bound fraction was extracted from the beads with Laemmli sample buffer. Unbound and bound proteins were analyzed by SDS-polyacrylamide gel electrophoresis followed by Coomassie Blue staining.

Fluorescence spectroscopy: Peptide concentration was determined by UV spectrophotometry with $\varepsilon_{330} = 4640\,M^{-1}\,cm^{-1}$ for the dansyl group.[39] Steady-state fluorescence measurements were carried out at 20 °C on a Perkin–Elmer (Beaconsfield, UK) LS-5B spectrofluorimeter. The buffer contained MOPS-NaOH (5 mM), NaCl (120 mM), pH 7.0. The peptide–protein binding experiments were carried out in the presence of $CaCl_2$ (5 mM) or in the presence of ethylenediaminetetraacetic acid (1 mM) for those experiments that required a Ca^{2+}-free buffer. Fluorescence emission spectra of the dansyl group were obtained by excitation at 330 nm. The wavelength shifts were estimated as changes of the wavelength of the mid-point at two-thirds the height of the spectral band. The binding of DNS–$p21^{145-164}$ to CaM, PCNA, and SET was quantitatively analyzed by using the two-state model[25] and assuming that the peptide is either free in solution or bound to the protein in a unique state. This model allows the estimation of the apparent dissociation constant, $K_{d,app}$. The fluorescence intensity increases in the presence of the target protein and allows an experimental estimate to be made of the characteristic change in intensity for the peptide when it is totally bound (I_{max}) from a double-reciprocal plot of $(I - I_0)/I_0$ versus [protein], where I is the fluorescence intensity upon binding to the target protein, and I_0 is the intensity of fluorescence of the free peptide at the same wavelength. The expression $(I - I_0)/(I_{max} - I_0)$ defines the fraction of peptide bound.

Circular dichroism spectroscopy: All measurements were carried out on a Jasco J-810 CD spectropolarimeter, in conjunction with a Neslab RTE 110 waterbath and temperature controller. CD spectra were the average of a series of ten scans made at 0.2-nm intervals. CD spectra of the same buffer (or in the presence of TFE or SDS, as described in the figure legends) without peptide were used as the baseline in all the experiments. The peptide concentration was obtained by quantitative amino acid analysis.

NMR spectroscopy: NMR spectra were recorded on a Bruker Avance spectrometer operating at 500 MHz. Samples were prepared at a peptide concentration of 2.5 mM in two solvents: neat water and water containing 20% TFE. The spectra were acquired at 288 K. Water-signal suppression was achieved by using the WATERGATE sequence.[40] Phase-sensitive DQF-COSY,[41] TOCSY,[42] and ROESY[43] were used for sequence-specific assignments. HSQC[44] and HMQC[45] experiments were performed to assign C_α chemical shifts. TOCSY and ROESY spectra were recorded by using the MLEV-17 spin-lock sequence. Mixing times for TOCSY spectra were 15 and 80 ms. Mixing times for ROESY experiments were 250 and 300 ms. The number of scans varied between 32 and 64, the number of t_1 increments between 512 and 1024; the number of points in the t_2 dimension was 2048. ^1H resonances were assigned by using standard procedures.[30]

Generation of structure models: The structure of the complex $p21^{145-164}$–CaM was constructed with the CHARMM program.[46] The starting structure of $p21^{145-164}$ was modeled as a canonical α helix and subjected to energy minimization. Superimposition of the α-helical conformation obtained for $p21^{145-164}$ on the bound-to-CaM conformation of a 26-residue synthetic peptide comprising the CaM

binding domain of skeletal MLCK peptide (Protein Data Bank accession number 2BBM)[34] yielded a preliminary model of the complex. After replacement of the original peptide by $p21^{145-164}$, the coordinates of the C_α atoms of the complex were fixed in the original positions and minimized by 1000 steps of Steepest Descents algorithm. Then 1000 additional steps of Steepest Descents and 10000 steps of the Adopted Basis Newton – Raphson algorithm were applied with the C_α atoms free. The $p21^{145-164}$ – CaM complex rendered an energy convergence similar to that obtained when the same procedures were applied to the original MLCK – CaM complex. The figures were produced by using the program MOLMOL.[47]

This work was supported by grants from EU Biotechnology to E.P.-P. (Grant nºs BIO4-CT97 – 2086, CICYT – FEDER 1FD97 – 0291-C02 – 01, and SAF01 – 2811) and MCyT to O.B (Grant nº SAF2000 – 0052). We thank Alicia García for excellent technical work.

[1] D. O. Morgan, *Annu. Rev. Cell Dev. Biol.* **1997**, *13*, 261 – 291.
[2] Y. Xiong, H. Zhang, D. Beach, *Cell* **1992**, *71*, 505 – 514.
[3] J. W. Harper, G. R. Adami, N. Wei, K. Keyomarsi, S. J. Elledge, *Cell* **1993**, *75*, 805 – 816.
[4] W. S. el-Deiry, T. Tokino, V. E. Velculescu, D. B. Levy, R. Parsons, J. M. Trent, D. Lin, W. E. Mercer, K. W. Kinzler, B. Vogelstein, *Cell* **1993**, *75*, 817 – 825.
[5] M. Gorospe, C. Cirielli, X. Wang, P. Seth, M. C. Capogrossi, N. J. Holbrook, *Oncogene* **1997**, *14*, 929 – 935.
[6] C. J. Sherr, J. M. Roberts, *Genes Dev.* **1999**, *13*, 1501 – 1512.
[7] J. LaBaer, M. D. Garrett, L. F. Stevenson, J. M. Slingerland, C. Sandhu, H. S. Chou, A. Fattaey, E. Harlow, *Genes Dev.* **1997**, *11*, 847 – 862.
[8] G. P. Dotto, *Biochim. Biophys. Acta* **2000**, *1471*, 43 – 56.
[9] R. W. Kriwacki, L. Hengst, L. Tennant, S. I. Reed, P. E. Wright, *Proc. Natl. Acad. Sci. U.S.A.* **1996**, *93*, 11504 – 11509.
[10] A. Rodriguez-Vilarrupla, Díaz, C., Canela, N., Rahn, H. P., Bachs, O., Agell, N., *FEBS Lett.* **2002**, *531*, 319 – 323.
[11] M. Taules, A. Rodriguez-Vilarrupla, E. Rius, J. M. Estanyol, O. Casanovas, D. B. Sacks, E. Perez-Paya, O. Bachs, N. Agell, *J. Biol. Chem.* **1999**, *274*, 24445 – 24448.
[12] J. M. Estanyol, M. Jaumot, O. Casanovas, A. Rodriguez-Vilarrupla, N. Agell, O. Bachs, *J. Biol. Chem.* **1999**, *274*, 33161 – 33165.
[13] J. M. Gulbis, Z. Kelman, J. Hurwitz, M. O'Donnell, J. Kuriyan, *Cell* **1996**, *87*, 297 – 306.
[14] M. Zhang, T. Yuan, *Biochem. Cell Biol.* **1998**, *76*, 313 – 323.
[15] A. Crivici, M. Ikura, *Annu. Rev. Biophys. Biomol. Struct.* **1995**, *24*, 85 – 116.
[16] K. T. O'Neil, W. F. DeGrado, *Trends Biochem. Sci.* **1990**, *15*, 59 – 62.
[17] K. T. O'Neil, H. R. Wolfe, Jr., S. Erickson-Viitanen, W. F. DeGrado, *Science* **1987**, *236*, 1454 – 1456.
[18] V. Esteve, S. Blondelle, B. Celda, E. Perez-Paya, *Biopolymers* **2001**, *59*, 467 – 476.
[19] W. L. DeLano, M. H. Ultsch, A. M. de Vos, J. A. Wells, *Science* **2000**, *287*, 1279 – 1283.
[20] E. J. Sundberg, R. A. Mariuzza, *Structure* **2000**, *8*, 137 – 142.
[21] C. Zwahlen, S. C. Li, L. E. Kay, T. Pawson, J. D. Forman-Kay, *EMBO J.* **2000**, *19*, 1505 – 1511.
[22] N. Canela, A. Rodriguez-Vilarrupla, J. M. Estanyol, C. Diaz, M. J. Pujol, N. Agell, O. Bachs, *J. Biol. Chem.* **2003**, *278*, 1158 – 1164.
[23] Z. Q. Pan, J. T. Reardon, L. Li, H. Flores-Rozas, R. Legerski, A. Sancar, J. Hurwitz, *J. Biol. Chem.* **1995**, *270*, 22008 – 22016.
[24] D. I. Zheleva, N. Z. Zhelev, P. M. Fischer, S. V. Duff, E. Warbrick, D. G. Blake, D. P. Lane, *Biochemistry* **2000**, *39*, 7388 – 7397.
[25] A. Fersht, *Structure and Mechanism in Protein Science*, W. H. Freeman and Company, New York, **1999**.
[26] J. Chen, R. Peters, P. Saha, P. Lee, A. Theodoras, M. Pagano, G. Wagner, A. Dutta, *Nucleic Acids Res.* **1996**, *24*, 1727 – 1733.
[27] S. E. Blondelle, J. M. Ostresh, R. A. Houghten, E. Perez-Paya, *Biophys. J.* **1995**, *68*, 351 – 359.
[28] L. Zhong, W. C. Johnson, Jr., *Proc. Natl. Acad. Sci. U.S.A.* **1992**, *89*, 4462 – 4465.
[29] M. Vilar, V. Esteve, V. Pallas, J. F. Marcos, E. Perez-Paya, *J. Biol. Chem.* **2001**, *276*, 18122 – 18129.
[30] K. Wüthrich, *NMR of Proteins and Nucleic Acids*, John Wiley & Sons, Inc., New York, **1986**.
[31] Y. Xiong, G. J. Hannon, H. Zhang, D. Casso, R. Kobayashi, D. Beach, *Nature* **1993**, *366*, 701 – 704.
[32] I. B. Roninson, *Cancer Lett.* **2002**, *179*, 1 – 14.
[33] R. W. Kriwacki, J. Wu, L. Tennant, P. E. Wright, G. Siuzdak, *J. Chromatogr. A* **1997**, *777*, 23 – 30.
[34] M. Ikura, G. M. Clore, A. M. Gronenborn, G. Zhu, C. B. Klee, A. Bax, *Science* **1992**, *256*, 632 – 638.
[35] D. R. Kellogg, A. Kikuchi, T. Fujii-Nakata, C. W. Turck, A. W. Murray, *J. Cell Biol.* **1995**, *130*, 661 – 673.
[36] K. Nagata, H. Kawase, H. Handa, K. Yano, M. Yamasaki, Y. Ishimi, A. Okuda, A. Kikuchi, K. Matsumoto, *Proc. Natl. Acad. Sci. U.S.A.* **1995**, *92*, 4279 – 4283.
[37] M. Miyaji-Yamaguchi, M. Okuwaki, K. Nagata, *J. Mol. Biol.* **1999**, *290*, 547 – 557.
[38] P. Villalonga, C. Lopez-Alcala, M. Bosch, A. Chiloeches, N. Rocamora, J. Gil, R. Marais, C. J. Marshall, O. Bachs, N. Agell, *Mol. Cell. Biol.* **2001**, *21*, 7345 – 7354.
[39] E. Perez-Paya, J. Dufourcq, L. Braco, C. Abad, *Biochim. Biophys. Acta* **1997**, *1329*, 223 – 236.
[40] M. Piotto, V. Saudek, V. Sklenar, *J. Biomol. NMR* **1992**, *2*, 661 – 665.
[41] M. Rance, O. W. Sorensen, G. Bodenhausen, G. Wagner, R. R. Ernst, K. Wuthrich, *Biochem. Biophys. Res. Commun.* **1983**, *117*, 479 – 485.
[42] A. Bax, D. G. J. Davis, *J. Magn. Reson.* **1985**, *65*, 355 – 360.
[43] A. Bax, D. G. Davis, *J. Magn. Reson.* **1985**, *63*, 207 – 213.
[44] G. Bodenhausen, D. J. Ruben, *Chem. Phys. Lett.* **1980**, *69*, 185 – 189.
[45] L. Müller, *J. Am. Chem. Soc.* **1979**, *101*, 4481 – 4484.
[46] B. R. Brooks, R. E. Bruccoleri, B. D. Olafson, D. J. States, S. Swaminathan, M. Karplus, *J. Comput. Chem.* **1983**, *4*, 187 – 217.
[47] R. Koradi, M. Billeter, K. Wuthrich, *J. Mol. Graphics* **1996**, *14*, 51 – 55.

Received: May 2, 2003 [F649]

